UNCLASSIFIED

AD NUMBER

AD473132

NEW LIMITATION CHANGE

TO

Approved for public release, distribution unlimited

FROM

No public or foreign release.

AUTHORITY

DTRA ltr., 6 May 99

THIS PAGE IS UNCLASSIFIED

AD 472132

GENERAL ATOMIC
DIVISION OF GENERAL DYNAMICS

GA-6693

COMPUTER EXPERIMENTS ON ION-MOLECULE REACTIONS

by

Fred A. Wolf

DDC
NOV 1 1965
DDC-IRA E

October 6, 1965

GENERAL ATOMIC

DIVISION OF

GENERAL DYNAMICS

JOHN JAY HOPKINS LABORATORY FOR PURE AND APPLIED SCIENCE

P.O. BOX 608, SAN DIEGO, CALIFORNIA 92112

GA-6693

COMPUTER EXPERIMENTS ON ION-MOLECULE REACTIONS

by

Fred A. Wolf†

Prepared for submission to
Journal of Chemical Physics

Sponsored in part by the
Defense Atomic Support Agency
Washington, D. C.
under Contract DA-49-146-XZ-354
and in part by the
U. S. Navy Electronics Laboratory
San Diego, California

†Consultant to General Atomic and Assistant Professor of Physics, San Diego State College, San Diego, California

October 6, 1965

ABSTRACT

A computer program has been developed which follows Light's phase-space theory of three-body ion-molecule reactions. The program predicts cross sections for 10 possible reaction branches as functions of the relative kinetic energy of the colliding particles in the range from thermal energies up to 20 eV. It also yields partial cross sections for the populations of the vibrational levels of the diatomic molecule in the product channel. Included in the results are reactions for the following ion-molecule pairs: $[O^+ + N_2]$, $[N^+ + O_2]$, $[O + N_2^+]$, $[He^+ + N_2]$, and $[(O^{18})^+ + O_2]$. The effects of varying the level of excitation, both vibrationally and electronically, of the reactants are presented. Increasing the excitation level always results in greater cross sections for reactions which are otherwise endothermic and slightly smaller cross sections for reactions which are otherwise exothermic.

All endothermic cross sections reach maximum values as functions of the barycentric kinetic energy of the reactants. All exothermic cross sections decrease with increasing barycentric kinetic energy at rates faster than predicted by the Gioumousis and Stevenson theory. This is due to the greater competition between the products for the available phase space which occurs at elevated energies. Good agreement is found between the theory and experiment in the high energy region above 5 eV and in some cases throughout the whole energy range. Disagreement is most pronounced for low energies. It is felt that this indicates the presence of a small activation energy or, in the case where the products differ from the reactants by a charge transfer $A^+ + BC \rightarrow A + BC^+$, the neglect of including resonance forces in the calculation.

CONTENTS

FIGURES

FIGURES (Cont'd.)

FIGURES (Cont' d.)

1. INTRODUCTION

Experimental data[1-4] giving cross sections as functions of the reactant ion energy, appearing in the literature on ion-molecule reactions, have up to now been compared only with the theory of Gioumousis and Stevenson (G and S).[5] This theory is based on the Langevin model which yields orbits of a charged particle moving in the induced dipole potential which exists between the charged and neutral particles. When the impact parameter is less than a certain critical value, an inward spiraling orbit takes place. Hence if the impact parameter is less than critical, a reaction can be expected to occur, whereas impact parameters greater than critical cannot give rise to reaction. This reaction cross section is given by

$$\sigma(E_{tr}) = \pi(2e^2\alpha/E_{tr})^{\frac{1}{2}}, \qquad (1)$$

where e is the charge of an electron, α is the polarizability of the neutral particle, and E_{tr} is the usual kinetic energy of the reduced mass particle in the center of mass coordinate system.

While this theory has been successfully compared to many of the experimental data, it has not been able to predict such features as the appearances of maxima in the cross section versus energy curves or the rapid fall off of the reaction cross sections with higher energy, nor has it been able to deduce what fraction of the products are in excited vibrational and electronic states. In fact, there is no way that the G and S theory can explain which of the products are most likely to be found after reaction or the fact that in some cases no reaction occurs at all.

This is not surprising when one realizes that this theory gives only an upper bound to the reaction cross section.[6] Hence one should not expect to find any "structure" in the cross section-energy curve predicted by it. Because calculations of cross sections for ion-molecule reactions are practically intractable quantum mechanically and because many experimental data indicate something other than that predicted by Gioumousis and Stevenson, we feel that the phase-space theory of Light[7] deserves special attention[8,9]. To study this theory we have investigated the following ion-molecule reactions:

$$O^+ + N_2 \rightarrow \text{products},$$

$$N^+ + O_2 \rightarrow \text{products},$$

$$(O^{18})^+ + O_2 \rightarrow \text{products},$$

$$O + N_2^+ \rightarrow \text{products},$$

$$He^+ + N_2 \rightarrow \text{products}. \qquad (2)$$

These reactions are of some importance in the atmosphere. Before giving the results we shall first review the Light theory.

2. DESCRIPTION OF THE LIGHT THEORY

Light's phase-space theory[7] is based upon the postulate that: "The probability of formation of any given product in a 'strong coupling' collision is proportional to the ratio of the phase space available to that product divided by the total phase space available with conservation of energy and total angular momentum." The strong coupling is necessary to ensure that the complex formed by the reactants "loses all memory" of its initial state, and consequently that its decomposition be governed by phase space available.

The classical three-particle phase-space element is the usual

$$d\Gamma = \prod_{i=1}^{3} d^3 r_i d^3 p_i \quad , \tag{3}$$

where r_i and p_i are the position and momentum coordinates of particle i. By separating out the center of mass motion, writing $\vec{J}_T = \vec{J}_{ORB} + \vec{J}_{ROT}$, and taking $\vec{J}_T$ to lie along the z-axis, we find after a Jacobian transformation, the reduced phase-space element

$$d\Gamma = \left(J_T^2 + J_{ROT}^2 - 2J_T J_{ZROT}\right)^{-\frac{1}{2}} J_T dJ_T dJ_{ZT} d\beta_T d\alpha_{ORB}$$

$$dE_T dt_T dJ_{ROT} dJ_{ZROT} d\alpha_{ROT} d\beta_{ROT} dE_{VIB} dt_{VIB} \quad , \tag{4}$$

where the symbol J refers to angular momentum, E refers to energy, t to time, α to the angle conjugate to J, and β to the angle conjugate to the Z component of J. The subscript T means total, ORB means orbital and refers to the orbital motion of the single particle about the molecule, ROT means rotational and refers to the rotation of the diatomic molecule about its mass center, and VIB means vibrational and refers to vibration of the diatomic molecule.[10] By noticing that the integrals over α_{ORB}, α_{ROT}, β_{ROT}, β_T, t_T, and t_{VIB} yield constants independent of channel and vibrational energy, we can write for the relevant phase space available with conservation of total energy E_T, vibrational energy E_{VIB}, and total angular momentum $\vec{J}_T$,

$$\Gamma = \iint \left[1 + \left(J_{ROT}/J_T\right)^2 - 2J_{ZROT}/J_T\right]^{-\frac{1}{2}} dJ_{ROT} dJ_{ZROT} \quad . \tag{5}$$

It should also be noted that the integral given by Eq. (9) of Reference 7 is incorrect, as suggested by Pechukas and Light in a later paper.[11] The correct expression is given by our Eq. (5).

The limits of integration of Eq. (5) are determined by the following physical constraints:

a. Since energy must be conserved we have

$$E_T = E_{tr}^{\,o} + E_v^{\,o} + E_{ROT}^{\,o} = E_{tr}^{\,i} + E_v^{\,i} + E_{ROT}^{\,i} - Q_{oi} \qquad (6)$$

where E_{tr} is the translational kinetic energy $\mu v^2/2$, μ is the reduced mass of the diatomic molecule in channel k, and $E_{ROT}^{\,k}$ is its rotational energy. This is given by

$$E_{ROT} = J_{ROT}^{\,2}/2I \ , \qquad (7)$$

where I is the moment of inertia of the diatomic molecule. The superscripts o and i refer to the input and ith output channel respectively, and Q_{oi} is the exothermicity for the reaction. Thus an endothermic channel will have a negative Q. Because E_{tr} must be positive, Eq. (6) yields for each channel i an upper bound on the rotational angular momentum

$$J_{ROT}^{\,2}/2I \leq E_T - E_v^{\,i} + Q_{oi} = \epsilon \ . \qquad (8)$$

b. Since the molecule in the output channel must be stable, we must also limit the molecule from dissociating rotationally. Therefore

$$J_{ROT}^{\,2}/2I < D_v^{\,i} \ , \qquad (9)$$

where $D_v^{\,i}$ is the dissociation energy of the diatomic molecule from the vibrational level v.

c. The final requirement is that the products must separate. When the products are an ion and a neutral particle, the effective one-dimensional central-field potential is given by

$$V(r) = - e^2\alpha/2r^4 + E_f b_f^{\,2}/r^2 \qquad (10)$$

where α is the polarizability of the neutral particle, E_f is the final translational kinetic energy, and b_f is the impact parameter for the products. This interaction potential can be expected to be physically valid only for long ranges. Clearly the short-range repulsion is not included; however, it would only be important for large values of the mass reduced orbital angular momentum, $J_{ORB}^2/2\mu = E_f b_f^2$. For low relative kinetic energies, the centrifugal barrier occurs in the region of the attractive induced dipole potential. For intermediate values of E_f, quantum mechanical resonance forces must be taken into account.[12] Present calculations are underway which include resonance potentials. The results will be reported soon for several pertinent ion-molecule reactions.

The charge-quadrupole interaction which leads to a potential varying as r^{-3} can be neglected on the basis that it is usually much smaller than the induced dipole-charge interaction. This has been investigated by Arthurs and Dalgarno.[13] Applying their calculation to $H_2 + H_2^+$ leads to the cross section

$$\sigma_{AD} = 1.08 \left(E_{tr}\right)^{-2/3} (\text{Å}^2) \quad , \tag{11}$$

where E_{tr} is the relative kinetic energy of the reactants in eV.

The G and S cross section for this reaction is

$$\sigma_{GS} = 15.08 \left(E_{tr}\right)^{-\frac{1}{2}} (\text{Å}^2) \; ; \tag{12}$$

hence, it is clear that the charge-quadrupole interaction is only important at extremely low energies, well below room temperature.

The restriction that the products must separate can be written very simply as

$$E_f \geq V(r^*) \quad , \tag{13}$$

where

$$r^* = \left(e^2\alpha/E_f b_f^2\right)^{\frac{1}{2}} \quad , \tag{14}$$

and

$$V(r^*) = \left|E_f b_f^2\right| \Big/ (2e^2\alpha) \tag{15}$$

are the position and value of the potential, respectively, for the centrifugal barrier. This can be converted into a condition which limits the range of values taken by J_{ZROT}.[14]

Using conditions a and c, we find for the total phase space available to products i in vibrational state v, the result

$$\Gamma_i(J_1, J_2, J_T, \epsilon) = I_1 + I_2\, S(-J_1) + I_3\, \mathrm{sgn}(J_T - J_2) + I_4\, S(J_1)\, \mathrm{sgn}(J_T - J_1) + I_5\, S(J_2 - J_T)\, S(J_T - J_1), \tag{16}$$

where in the above

$$S(A - B) = \begin{cases} 1, & A > B \\ 0, & A < B \end{cases}, \qquad \mathrm{sgn}(A - B) = \begin{cases} +1, & A > B \\ -1, & A < B \end{cases}, \tag{17}$$

and

$$I_1 = (8\mu^2 e^2 \alpha)^{1/4} \int_{|J_1|}^{J_2} \left(\epsilon - J_{ROT}^2/2I\right)^{1/4} dJ_{ROT},$$

$$I_2 = J_T|J_1| + \frac{1}{2} J_1^2,$$

$$I_3 = -J_T J_2 + \frac{1}{2} J_2^2,$$

$$I_4 = J_T|J_1| - \frac{1}{2} J_1^2,$$

$$I_5 = -J_T^2. \tag{18}$$

The values J_1 and J_2 correspond to the roots X_1 and X_2 given in Reference 7. Briefly, they are bounds on the values that J_{ROT} can assume when the inequality $E_f \geq V(r^*)$ is applied. They are given by

$$J_i = (2I\epsilon)^{\frac{1}{2}} X_i , \qquad i = 1, 2 , \tag{19}$$

and always satisfy the inequality $J_2 \geq |J_1|$. The total phase space available to all products is given by summing Γ_i over both vibrational and product (electronic) states.

$$\Gamma(E_T, J_T) = \sum_i \sum_v \Gamma_i(J_1, J_2, J_T, \epsilon) . \tag{20}$$

By not restricting Γ through use of condition b, we are including the phase space available to rotational dissociation.

Since the product channel contains a molecule, the product phase space available must be restricted by condition b. Writing $J_3 = (2ID_v^i)^{\frac{1}{2}}$ for brevity, we find for the product phase space

$$\begin{aligned}\Gamma_i'(J_1, J_2, J_T, \epsilon) = {} & \Gamma_i(J_1, J_2, J_T, \epsilon)\, S(J_3-J_2) \\ & + \Gamma_i(J_1, J_3, J_T, \epsilon)\, S(J_2-J_3)\, S(J_3-|J_1|) \\ & + [(2J_TJ_3-J_T^2)\, S(J_3-J_T) + J_3^2\, S(J_T-J_3)] \\ & \times S(-J_1)\, S(|J_1|-J_3) .\end{aligned} \tag{21}$$

The probability for the production of molecule i in the vth vibrational state is then given by

$$P(E_T, J_T, E_v^i) = \Gamma_i'/\Gamma(E_T, J_T) . \tag{22}$$

The cross section for this production is then

$$\sigma(E_{tr}^o, i, v) = 2\pi \int_o^{b_{max}} P(E_T, J_T, E_v^i)\, bdb , \tag{23}$$

where b is the impact parameter in the reactant channel and

$$b_{max} = \left(2e^2\alpha/E_{tr}^{o}\right)^{1/4} .$$

By using Eq. (23), we are assuming that the initial energy and angular momentum of rotation of the reactant molecule is negligible in comparison with the total energy and total angular momentum respectively. This allows us to take $J_T^2 = 2\mu E_{tr}^{o} b^2$. We point out that if P = 1, the cross section reduces to that predicted by the G and S theory; therefore, the phase-space theory enables us to predict what fraction of the total reaction cross section results in the production of a particular product channel i and vibrational state v.

The cross section for dissociation is found by subtracting the sum of the formation cross sections from the maximum, or

$$\sigma_{DISS} = \pi b_{max}^2 - \sum_i \sum_v \sigma\left(E_{tr}^{o}, i, v\right) . \qquad (24)$$

Our calculations have been carried out on a fast computer, using an expanded version of Light's original program to include 10 output channels. This includes a sub-program which yields the roots X_1 and X_2 of Eq. (19) in Reference 7 and calculates the integral I_1 by a simple numerical quadrature.

Our calculations make use of many data already available in the literature on atomic and molecular constants. Molecular potential energy curves, interatomic separations, dissociation energies, and vibrational energy levels, when given, were taken from the work of Gilmore.[15] Atomic polarizabilities were taken from the work of Parkinson,[16] and molecular polarizabilities were obtained from the experimental results of Rothe and Bernstein[17]. In all cases, vibrational levels were obtained using the formula[18]

$$E_v^{k} = (v + 1/2)\, h\nu_k - (v + 1/2)^2 \left(h\nu_k\right)^2/4\, D_e^{k} , \qquad (25)$$

where D_e^{k} is the dissociation energy from the bottom of the potential well of the product molecule k and fitting the frequencies ν_k to the potential energy curves given by Gilmore.

3. DISCUSSION OF THE RESULTS

The results of the calculations are shown in Figures 1 through 19. We have plotted cross sections in units of 10^{-16} cm^2 = 1 Å^2 versus the incoming relative kinetic energy of the reactants, $\mu v^2/2$, in eV units. For most of the energy range shown, a simple conversion from barycentric to laboratory ion energies is found by writing

$$E_{lab} = (m/\mu)\, E \quad , \tag{26}$$

where m is the incoming ion's mass and μ is the reduced mass of the reactants. For example, in Figure 1 the incoming reduced mass is $\mu = 16 \cdot 28/44$ amu, while the ion's mass is 16. Hence $E_{lab} = 1.57\, E$.

The straight negative sloped line labeled G and S in all of the figures represents the Gioumousis and Stevenson cross section for each set of reactants. Thus it appears as shown when plotted on the log-log graph. Furthermore, this cross section is the maximum obtainable when the induced dipole potential is used. By summing over all production cross sections, one obtains the G and S result.

Each curve, unless otherwise indicated, represents a composite in that it is a sum over all possible vibrational levels of the diatomic molecule in the output channel depicted. Thus Curve A1 in Figure 2 represents the total cross section for $NO^+(X\ ^1\Sigma^+)$ production. Figure 5 shows the vibrational distribution of the product A1.

Curves A2 and A3 of Figure 2 represent, respectively, the production of the excited neutral states $N(^2D)$ and $N(^3P)$ together with $NO^+(X\ ^1\Sigma^+)$. Since these reactions are endothermic, their cross sections are zero at low energies. Curve A of Figure 1 is the sum of A1, A2, and A3, and thus represents the total $N + NO^+$ production.

Curve B of Figure 1 represents the cross section for production of the same products as the reactants. For low energies, this cross section is non-reactive in that the products are also in the same vibrational state as the reactants. For higher energies, however, higher vibrational states will appear. This effect can be seen in Figure 5, which shows the vibrational distribution of the cross section for the production of $NO^+(X\ ^1\Sigma^+$ v=0, 1, ..., 11). In all the figures, at higher energies all vibrational levels are excited and the cross sections are seen to approach each other

asymptotically. Low-energy cross sections for particular vibrational levels only appear for those vibrational levels which are exothermic.

Comparing Figures 7 and 10, we see that for low energies, agreement is best for the reaction

$$N^+(^3P) + O_2(X\ ^3\Sigma_g^-\ v=0) \rightarrow O(^3P) + NO^+(X\ ^1\Sigma^+) \quad ,$$

while for energies above 5 eV, the experimental results agree with the total NO^+ production (the sum of Curves A1 through A6, represented as A on Fig. 7). We point out that the above reaction is more than 6-eV exothermic, and hence one may not expect to find any important effects, due to activation energies. The other reactions, A2 through A6 in Figure 10, are not as exothermic (A5 and A6 are endothermic); therefore, if activation is present, these reactions may not be observed at low energies. This could explain the good agreement of experimental results with A1 at low energies. At higher energies, the experimental results best fit the total NO^+ production shown as A in Figure 7. This agreement is reasonable in light of our previous discussion of phase-space competition at higher energies.

Discrepancies loom large, as a usual rule, whenever a resonant charge-transfer process is observed to take place; i.e., our results yield cross sections for rearrangement resulting in charge transfer which is usually smaller than observed experimentally. By taking into account resonance forces, we hope to be able to predict cross sections for low-energy charge transfer which give better agreement with experiment.[19] This will appear in a forthcoming paper. In the event that the reactant channel "sees" a resonance force, we could expect to find total cross sections which would exceed the G and S maximum.[12] In the event of actual rearrangement, the results seem promising. Agreement is expected to be best when the output channels are highly exothermic, i.e., when the effects of any activation energy are expected to be small. Thus, see the results for the reaction $N^+ + O_2 \rightarrow O + NO^+$. Here (Fig. 7) good agreement is found between theory and experiment throughout the energy range shown.

The most significant feature of the theory is the fact that our results yield cross sections for exothermic reactions which fall off faster with increasing barycentric kinetic energy than that predicted by Gioumousis and Stevenson when the energy exceeds 5 eV or so. This is in good agreement with experimental measurements[2,3,20,21] (witness Figs. 1, 7, 10, and 16). Our results indicate that this is due to phase-space competition. As the incoming energy increases, more channels open for the reaction path to follow. Thus each channel shares in the output. Finally, when the incoming energy is high enough, the exothermicities become small portions

of the total available energy. Hence all products become, roughly, equally likely. The small value for each cross section is attributed to the fact that more phase space is available to dissociated products at high energies than to stable vibrating molecules, since statistically a continuous energy distribution wins out over a discrete one.

The disagreement at low energies is significant and indicates either that an activation energy and/or "selection rule" restriction is in operation. Bates and Lynn point out[22] that even though a reaction may be favorable energetically, it may be ruled out if an electronic transition is required to "make it go". Thus they would predict low cross sections for asymmetric resonant systems. In the reaction $O^+ + N_2 \rightarrow NO^+ + N$ (Fig. 1), this is, however, not the case. The dissociated products and reactants match, i.e., $O^+ + N_2 \rightarrow O^+ + N + N \leftarrow NO^+ + N$, hence no electronic transition is required. Thus we are at a loss to explain the experimental data on this basis. Recently, Schmeltekopf and his associates at the National Bureau of Standards, Boulder, Colorado,[23] observed an increase of about a factor of 20 in the reaction rate for $O^+ + N_2 \rightarrow NO^+ + N$ when the N_2 was initially in a higher vibrational state. Our results are shown in Figures 4 and 6. More vibrational levels are excited in the NO^+ channel as a result of increasing the reactant vibrational energy. The measured results in this case do seem to agree with that predicted here, thus confirming the speculation that the theory best fits reactions which are strongly exothermic.

The results predicted by the reaction (Figs. 16-18)

$$He^+ + N_2 \rightarrow He + \left(N_2^+\right)^* \rightarrow He + N + N^+ \qquad (27)$$

deserve special mention. Here there is enough ionization energy available so that the dissociative reaction appears as an exothermic channel with the cross section increasing with decreasing energy. This is in contrast to any of the other cases shown, where dissociation, being an endothermic channel, does not take place until the translational kinetic energy exceeds the energy defect. Our results for dissociative charge transfer in this case fall much below the experimental results because the process is one in which resonance forces are probably quite large. Thus the accidental resonance reaction

$$He^+(^2S) + N_2(X\ ^1\Sigma_g^+\ v=0) \rightarrow He(^1S) + N_2^+(C\ ^2\Sigma_u^+\ v=4) + 0\ eV \qquad (28)$$

could predominate, as may be deduced from the theory of Rapp and Francis.[19] The phase-space theory as presented will always predict cross sections smaller than the G and S theory, and such a reaction as

(28) constitutes statistically a small part of the total Gioumousis and Stevenson cross section. It is, however, of interest to see the vibrational distribution of the output cross section for this reaction, and this is shown in Figure 18. By including resonance forces, we might expect the cross section for production of the v=4 level of N_2^+ C $^2\Sigma_g^+$ to be much larger than shown here. The potential energy curve crossing[15] of the $^4\Pi_u$ state with the C $^2\Sigma_u^+$ state would then lead to dissociation of the N_2^+ molecule[24].

We have also calculated cross sections for the reactions $N_2^+ + O$ and $(O^{18})^+ + O_2$. The former are shown in Figures 13 through 15 and the latter in Figure 19. The latter reaction is of interest for future experimentation, since it predicts a rather simple isotope effect. If we consider reactions of the type $A^+ + B_2$, we have as possible products

(a) $A + B_2^+$

(b) $AB + B^+$ (2 ways to form this)

(c) $AB^+ + B$ (2 ways to form this)

(d) $A^+ + B_2$

Consider products (a) and (b). If A is an isotope of B, the reaction for (b) will occur statistically twice as many times as that for (a). Hence rearrangement charge transfer (b) for the reaction $(O^{18})^+ + O_2 \rightarrow O + (O^{16}O^{18})^+$ will occupy twice the phase space available to simple charge transfer (a). Thus this reaction should prove a good test for the phase-space theory.

ACKNOWLEDGMENTS

It is a great pleasure to acknowledge the generous support offered by the U. S. Navy Electronics Laboratory during the summer of 1965. The author is most grateful to the above institution for allowing him use of their Control Data 1604 computer to carry out the calculations. Preliminary calculations were carried out on the University of California's Western Data Processing Center's IBM 7090-7094 system through use of their participating institutes' s teleprocessing system at San Diego State College.

Many enlightening discussions were held with Drs. M. Fineman, R. F. Stebbings, and J. W. McGowan of General Atomic, and Professor J. C. Light of the University of Chicago.

The author gratefully acknowledges receiving a preliminary computer program from Professor Light, and wishes to thank Dr. Stebbings and Professor Giese for permission to use unpublished data.

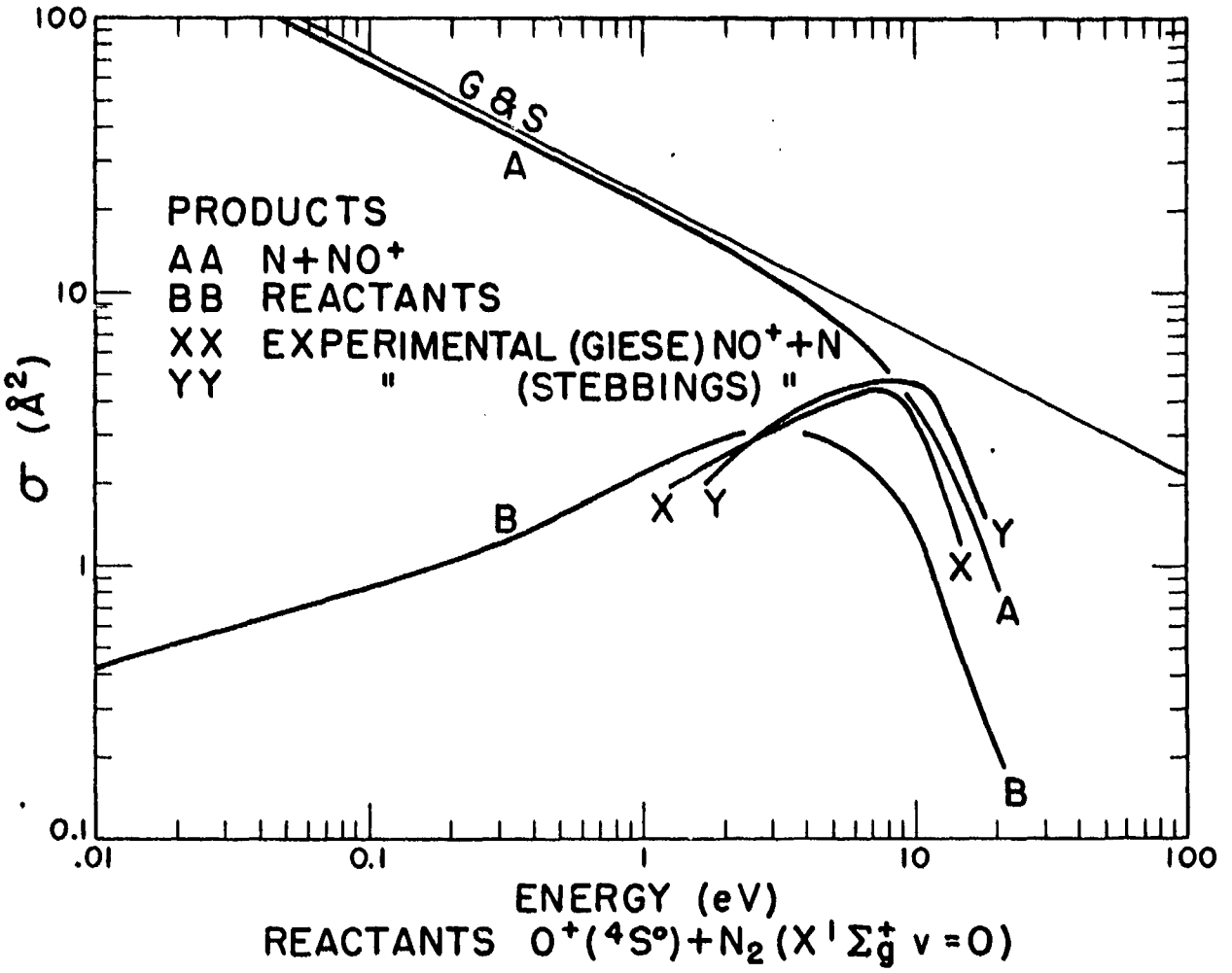

Fig. 1--Production of NO^+ from the reaction $O^+ + N_2$. The experimental NO^+ production results of Giese[21] and of Stebbings et al.[2] are shown by curves XX and YY respectively.

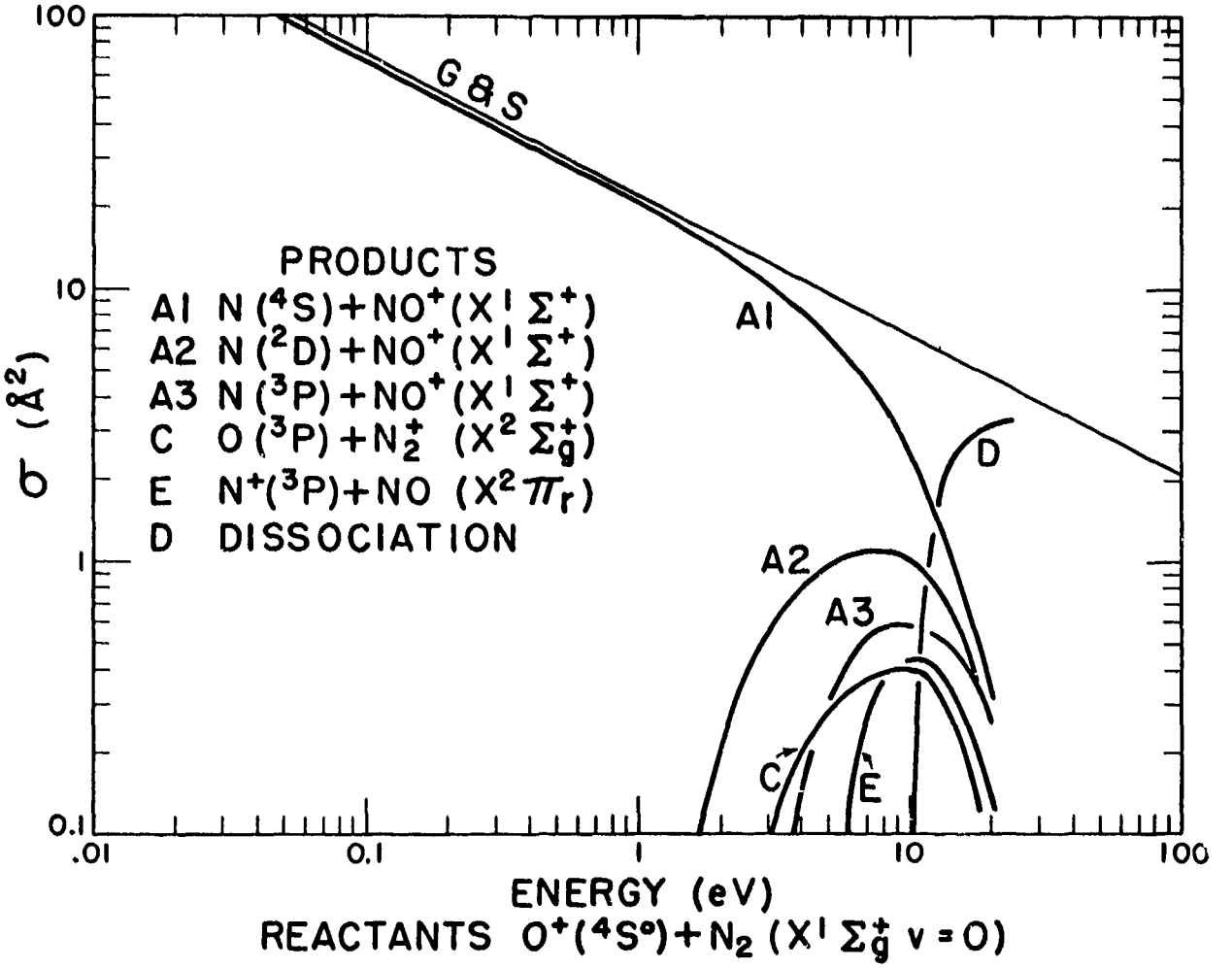

Fig. 2--Electronic distribution of the products born of the reaction $O^+ + N_2$. The products involved in dissociation (D) are probably 2N + O^+. The theory does not always predict which particle is ionized.

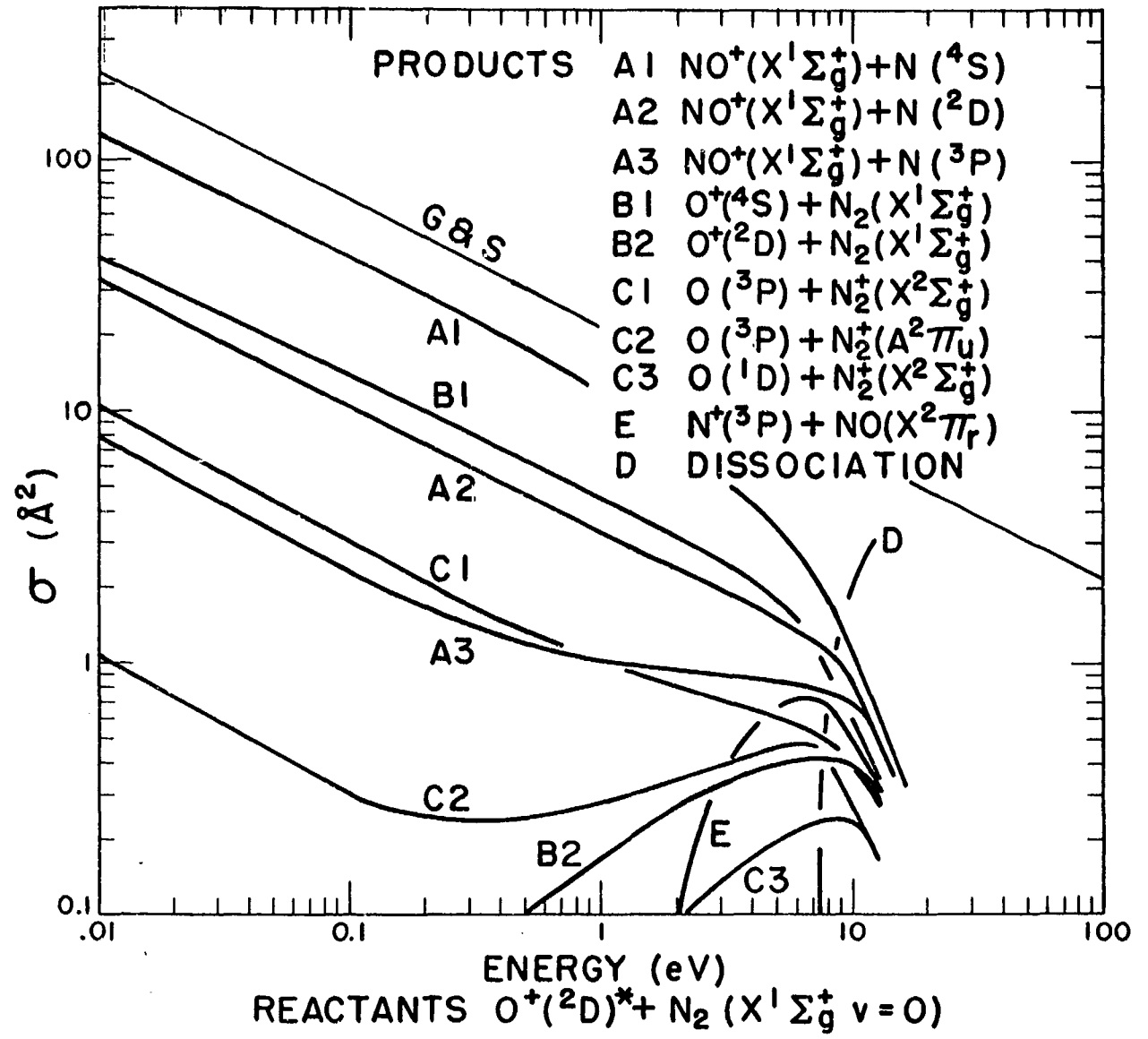

Fig. 3--Electronic distribution of the products from the reaction $(O^+)^*$ (^2D) + NO^+. The increase in the number of products follows from the greater energy available when one of the reactants is in an excited state. More channels are exothermic and therefore competitive for the available phase space.

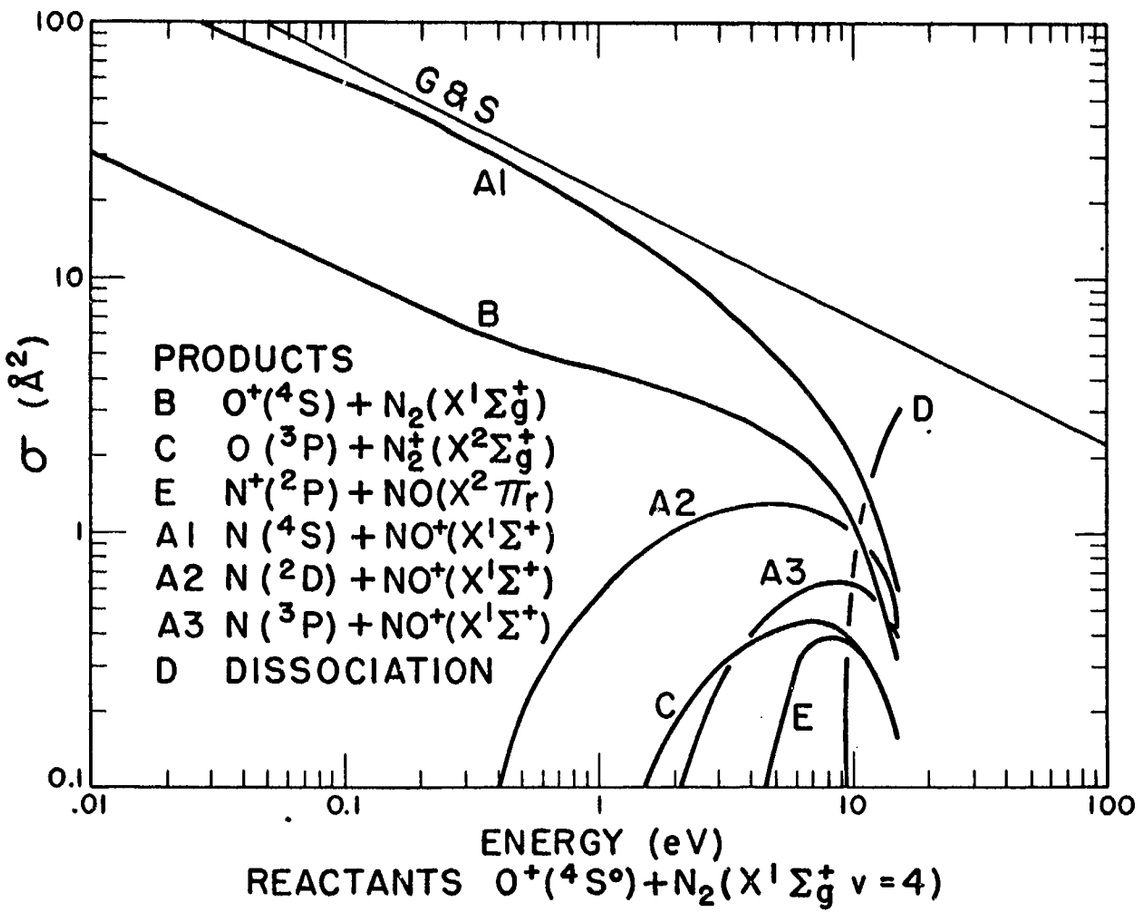

Fig. 4--Electronic distribution of the products from the reaction of $O^+ + N_2$ (v=4). The increased vibrational excitation of the reactant molecule produces a larger cross section (de-excitation) for formation of $O^+ + N_2$ (same products as reactants) because the de-excitation is exothermic.

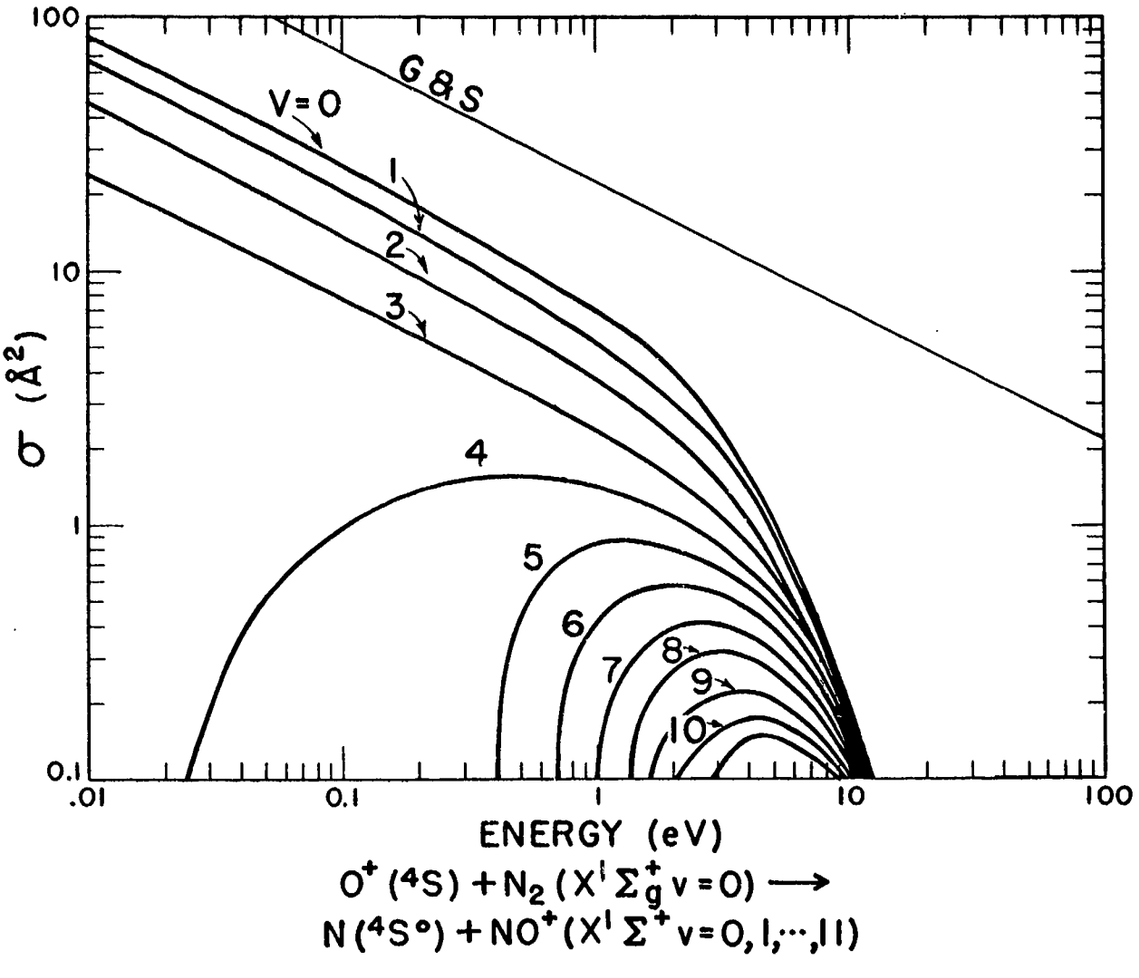

Fig. 5--Vibrational distribution of the products NO^+ (v=0, 1, ..., 11) + N from channels v=0, 1, 2, 3 are exothermic. Channels $v \geq 4$ are endothermic.

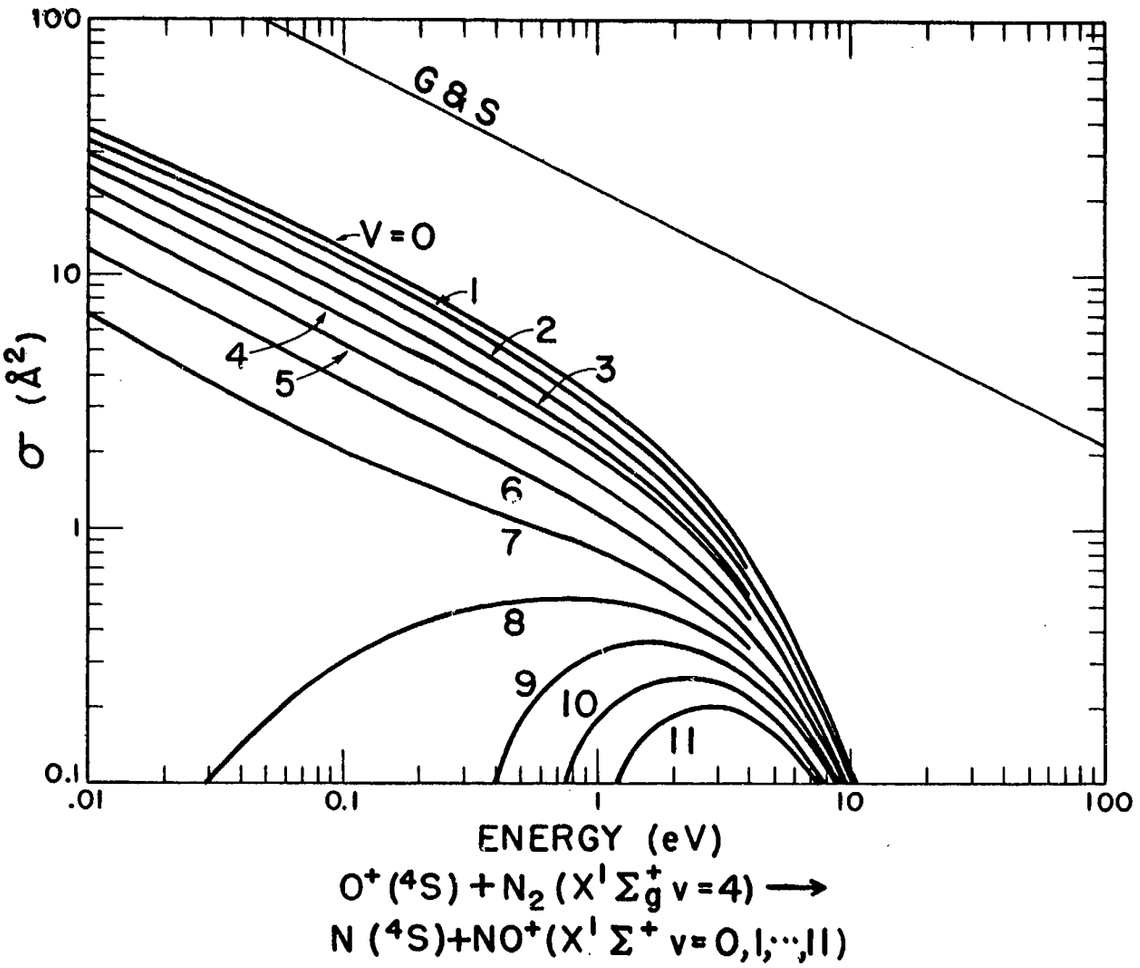

Fig. 6--Vibrational distribution of the products NO^+ (v=0, 1, ..., 11) + N from the reaction $O^+ + N_2$ (v=4). Channels $v \leq 7$ are exothermic, $v > 7$ are endothermic.

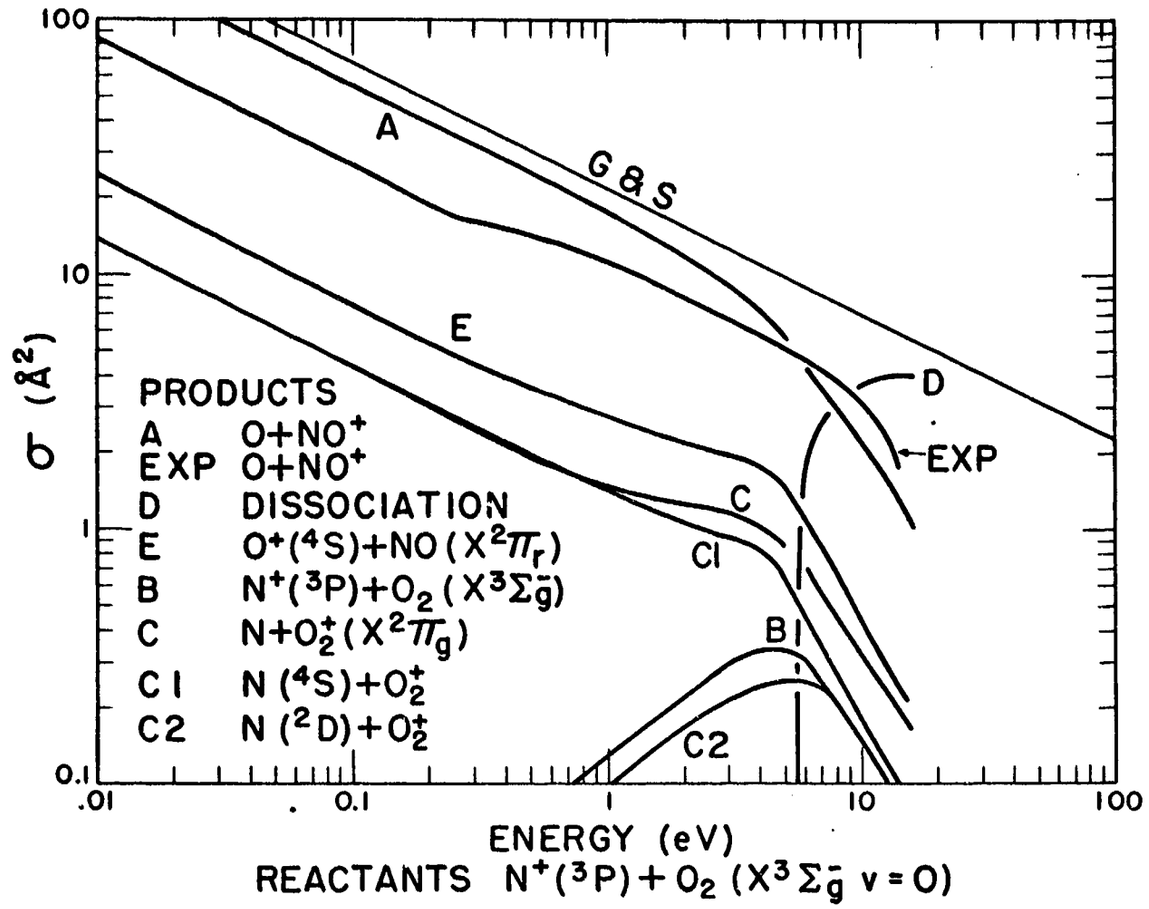

Fig. 7--Products NO^+, O^+, O_2^+ from the reaction $N^+ + O_2$. The experimental results shown are those of Stebbings et al.[2] Extrapolation is made to the low-energy experimental data of Fehsenfeld et al.[20]

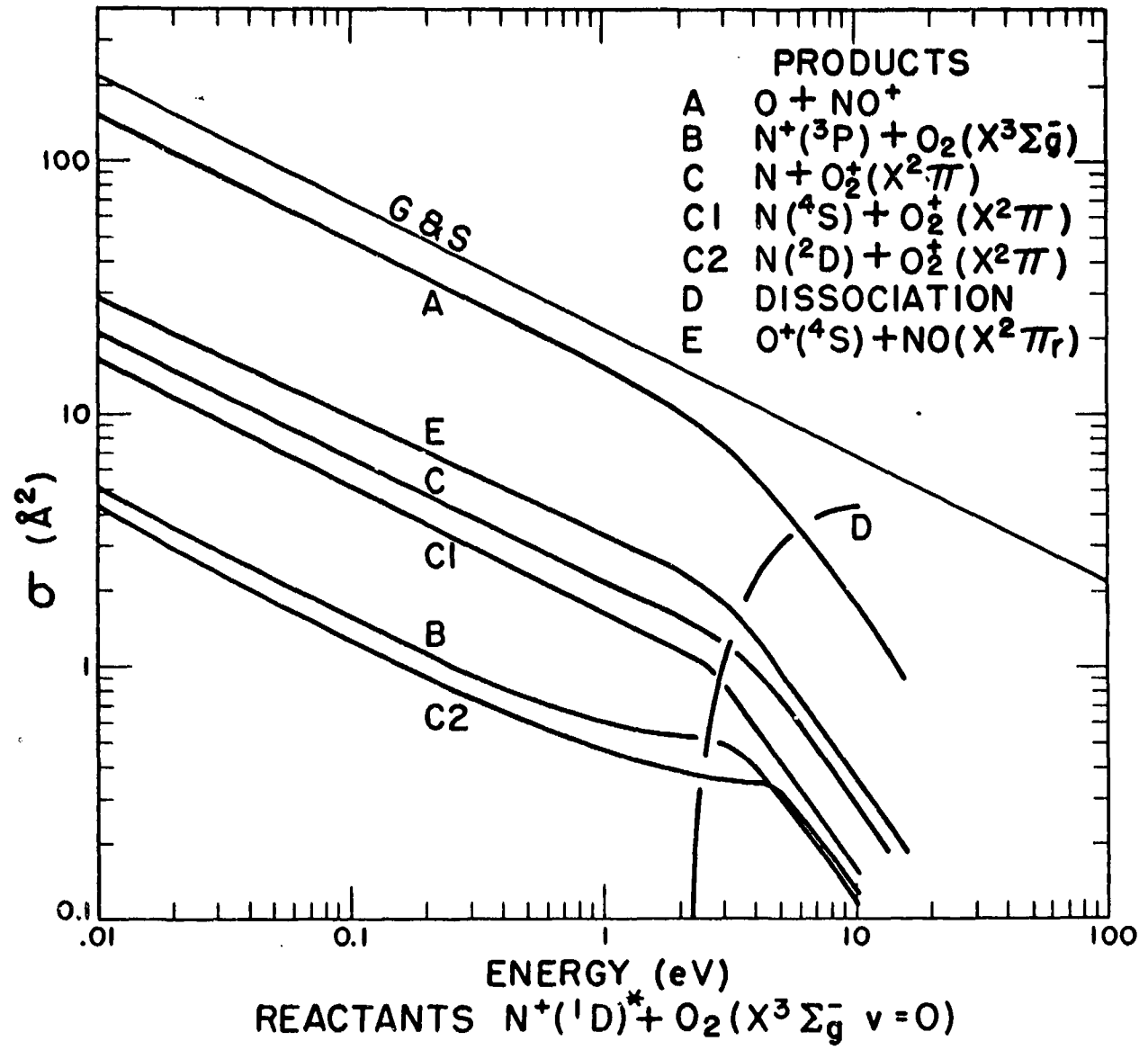

Fig. 8--Product distribution NO^+, N^+, O_2^+ and O^+ from the reaction $(N^+)^*$ + O_2. The de-excitation cross section is given by B.

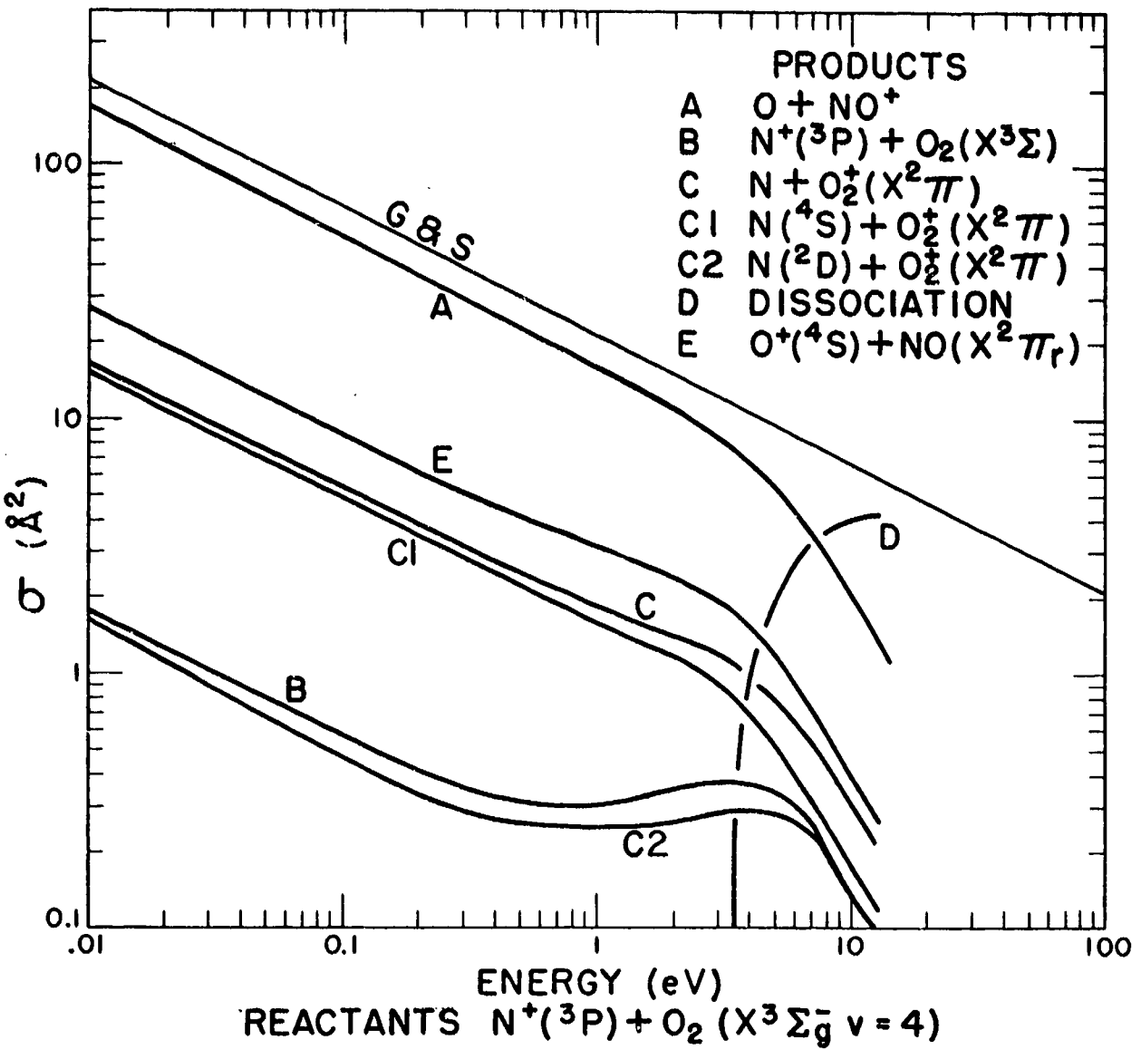

Fig. 9--Product distribution NO^+, N^+, O_2^+, and O^+ from the reaction $N^+ + O_2$ (v=4)

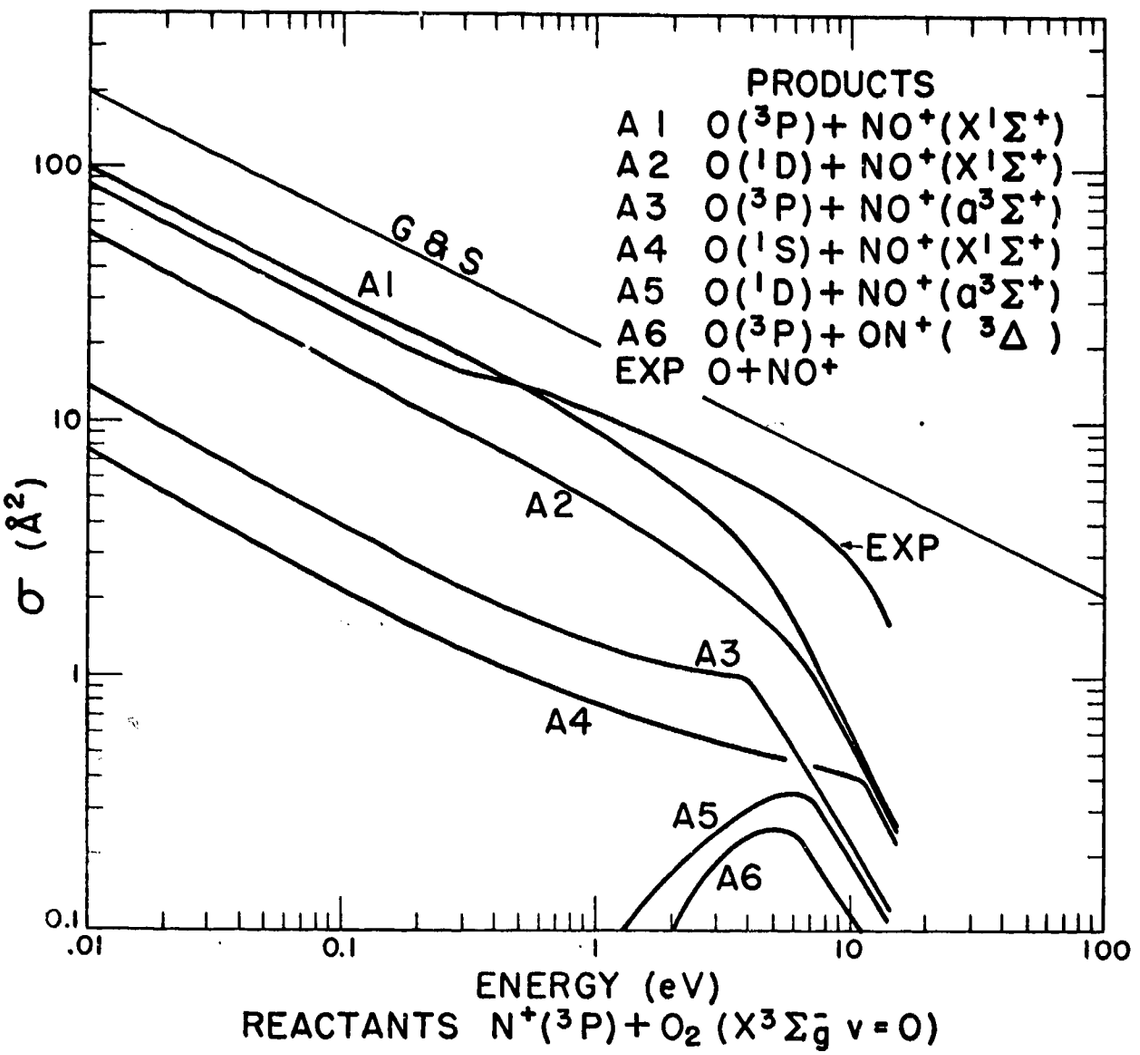

Fig. 10--Electronic distribution of the products $O + NO^+$ from the reaction $N^+ + O_2$. The experimental results are those of Stebbings et al.[2] at higher energies. These have been extrapolated to the room temperature data of Fehsenfeld et al.[20]

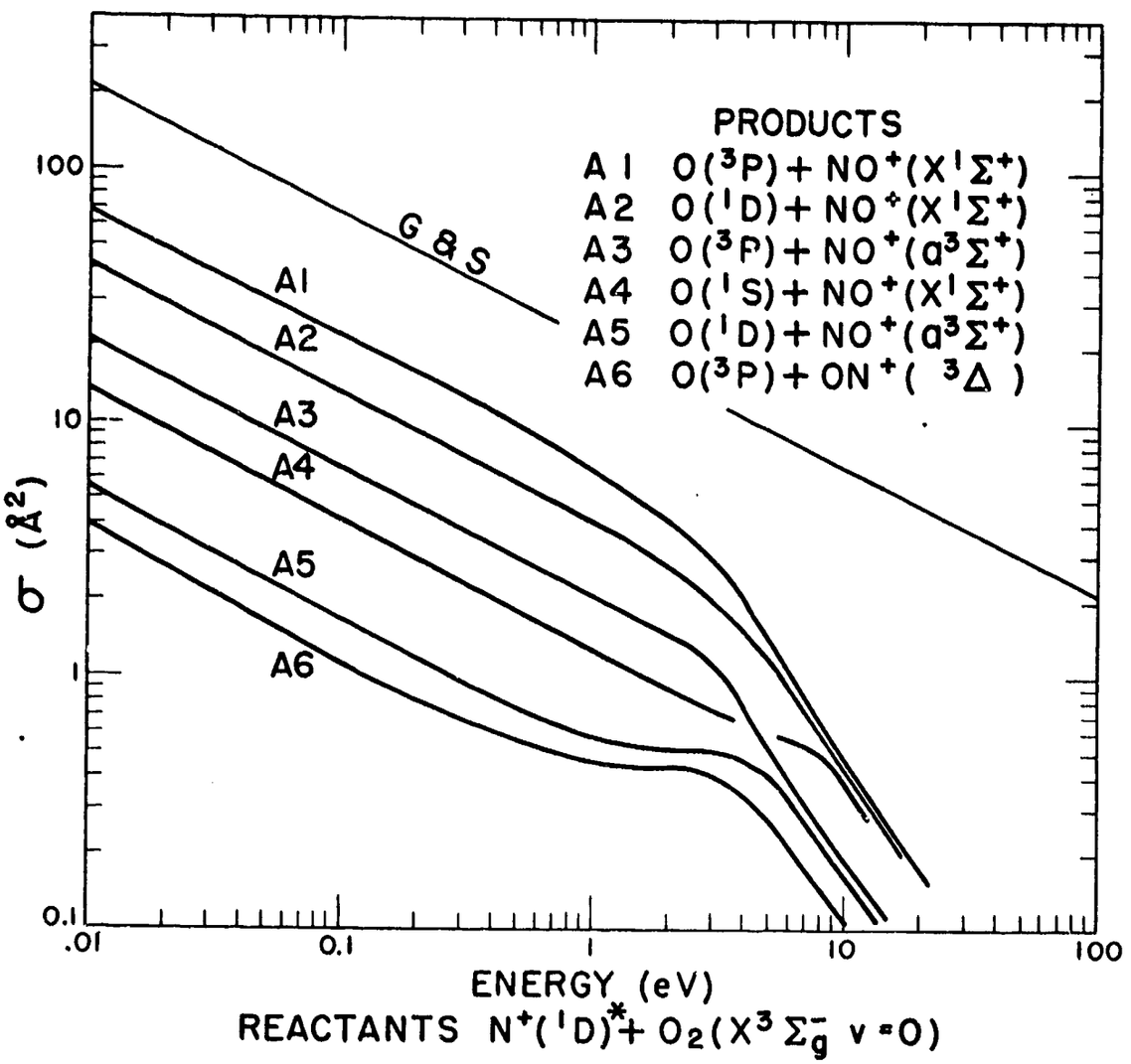

Fig. 11--Electronic distribution of the products $O + NO^+$ from the reaction $(N^+)^* + O_2$

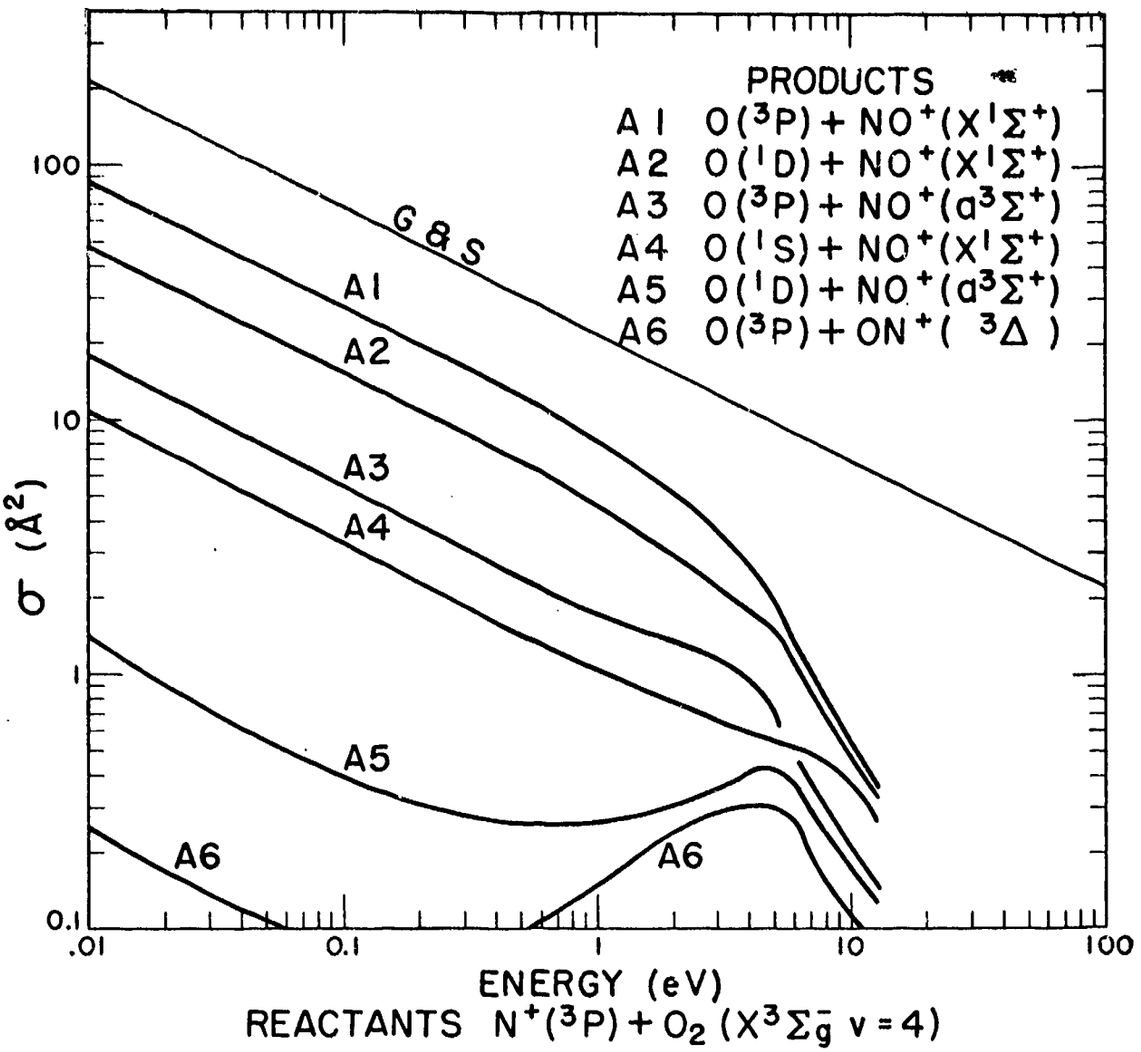

Fig. 12--Electronic distribution of the products $O + NO^+$ from the reaction $N^+ + O_2$ (v=4)

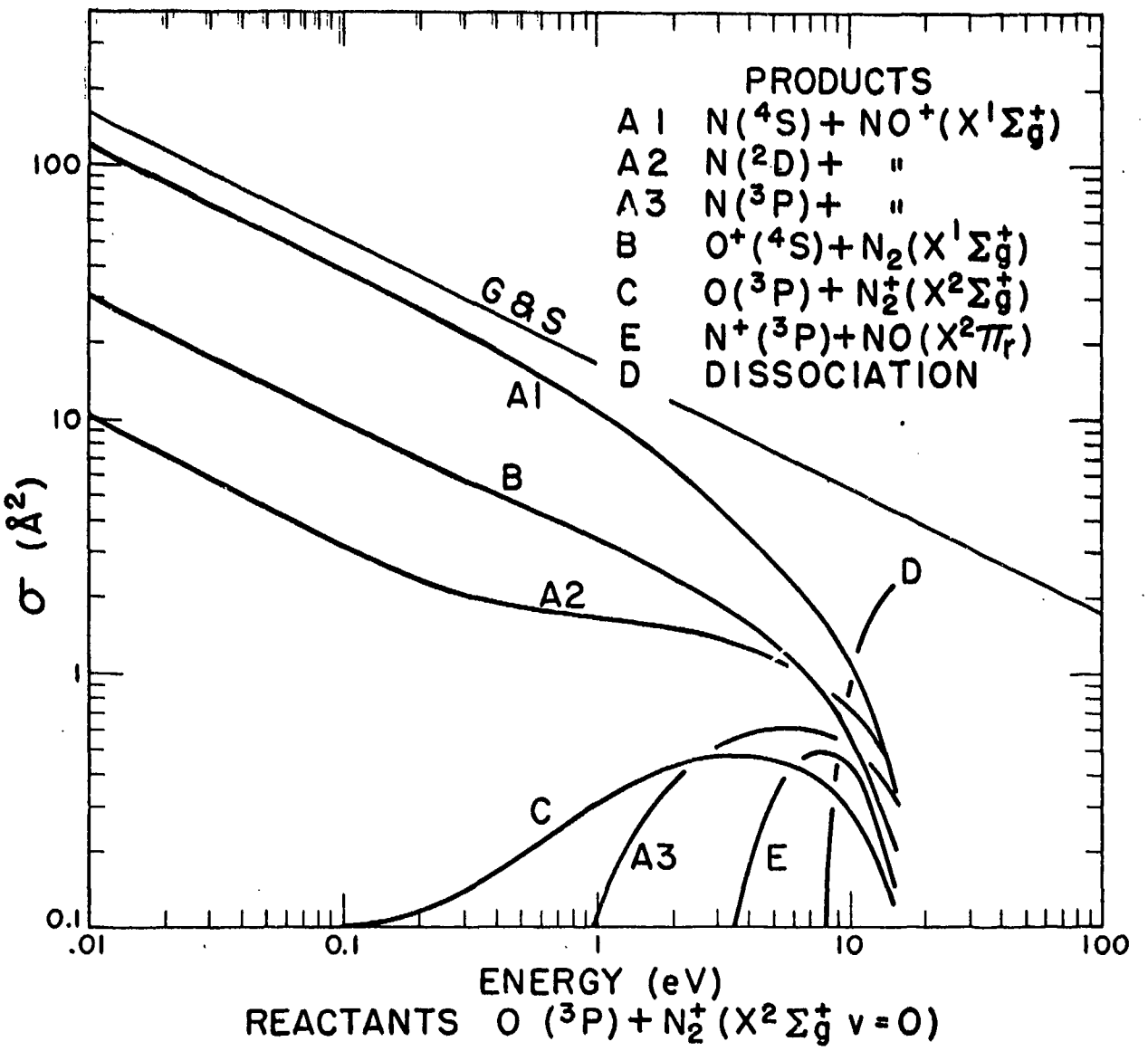

Fig. 13--Product distribution NO^+, O^+, N_2^+, and N^+ from the reaction $O + N_2^+$

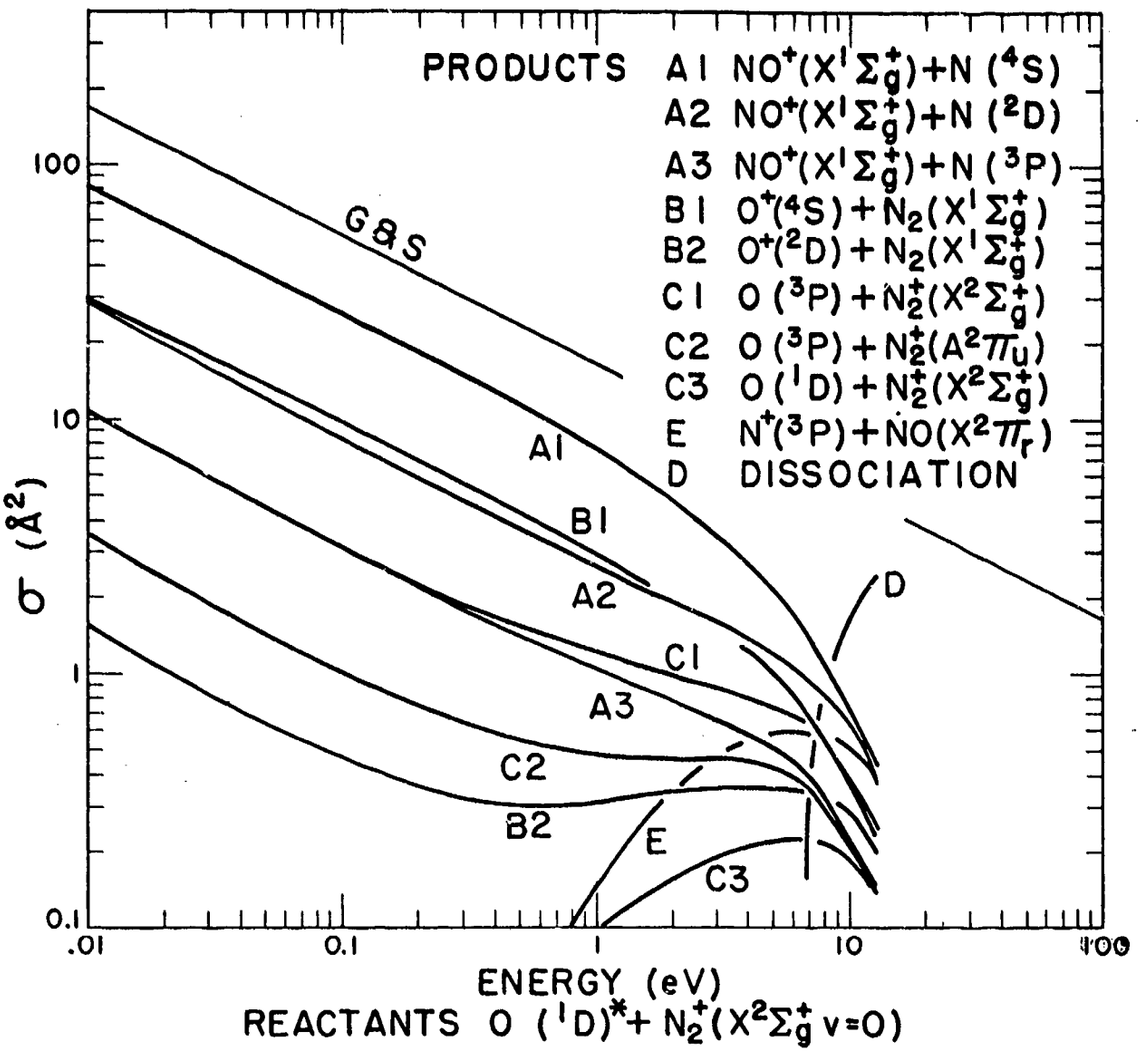

Fig. 14--Product distribution NO^+, O^+, N_2^+, and N^+ from the reaction $O^* + N_2^+$

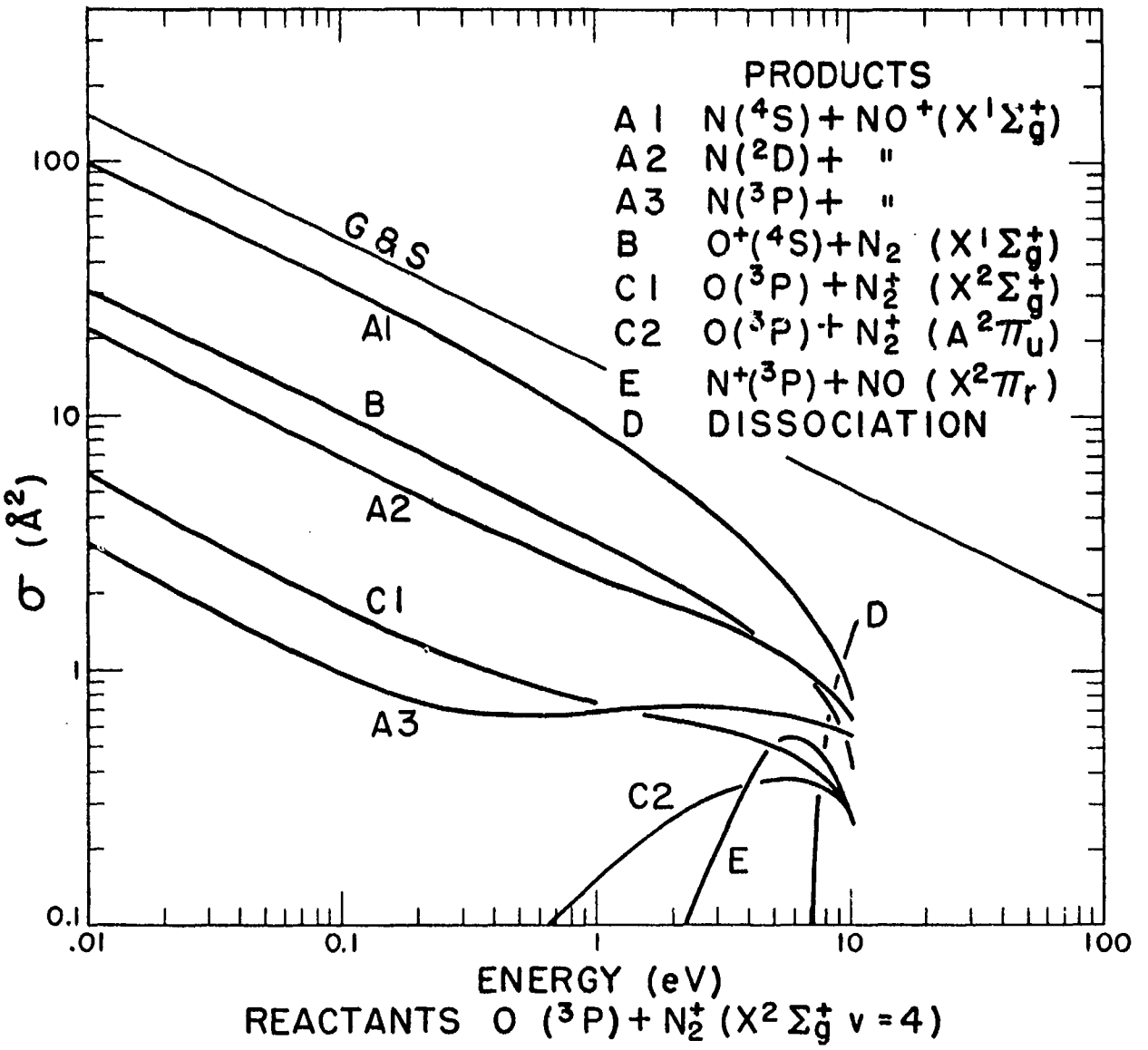

Fig. 15--Product distribution NO^+, O^+, N_2^+, and N^+ from the reaction $O + N_2^+$ (v=4)

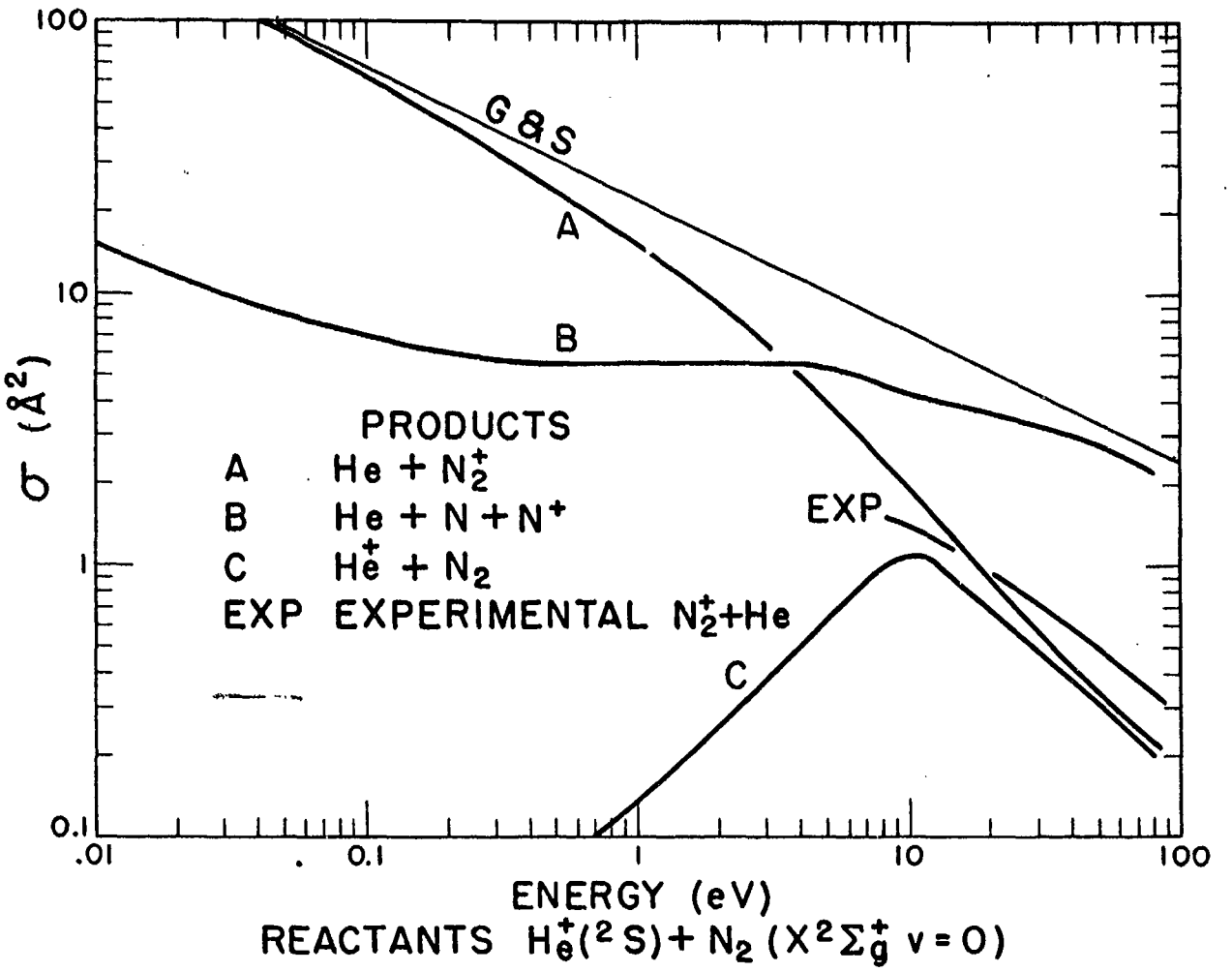

Fig. 16--Product distribution N_2^+, N^+, and He^+ from the reaction $He^+ + N_2$. The experimental data for N_2^+ production are taken from Stebbings et al.[3]

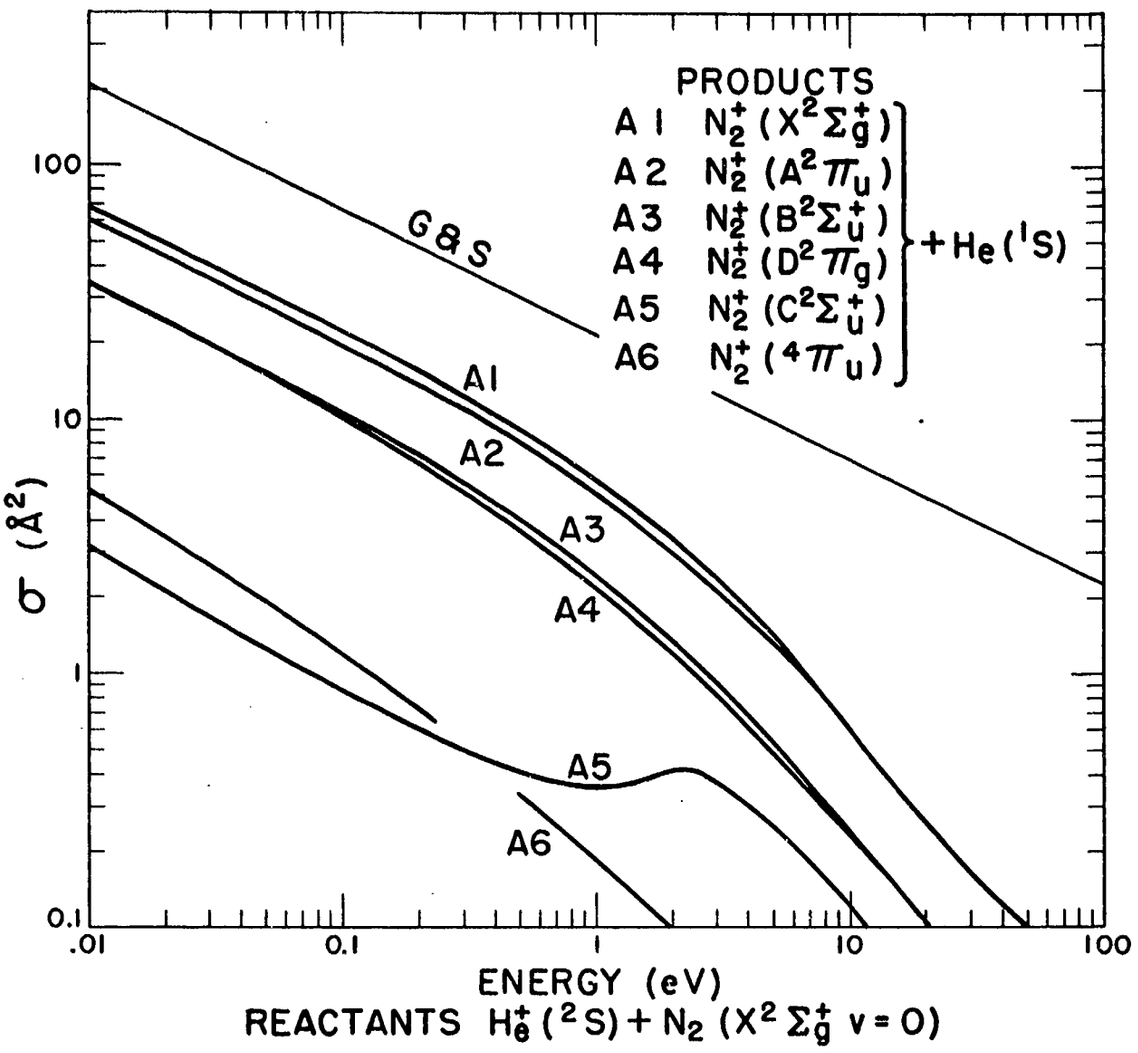

Fig. 17--Electronic distribution of the products He + N_2^+ from the reaction $He^+ + N_2$

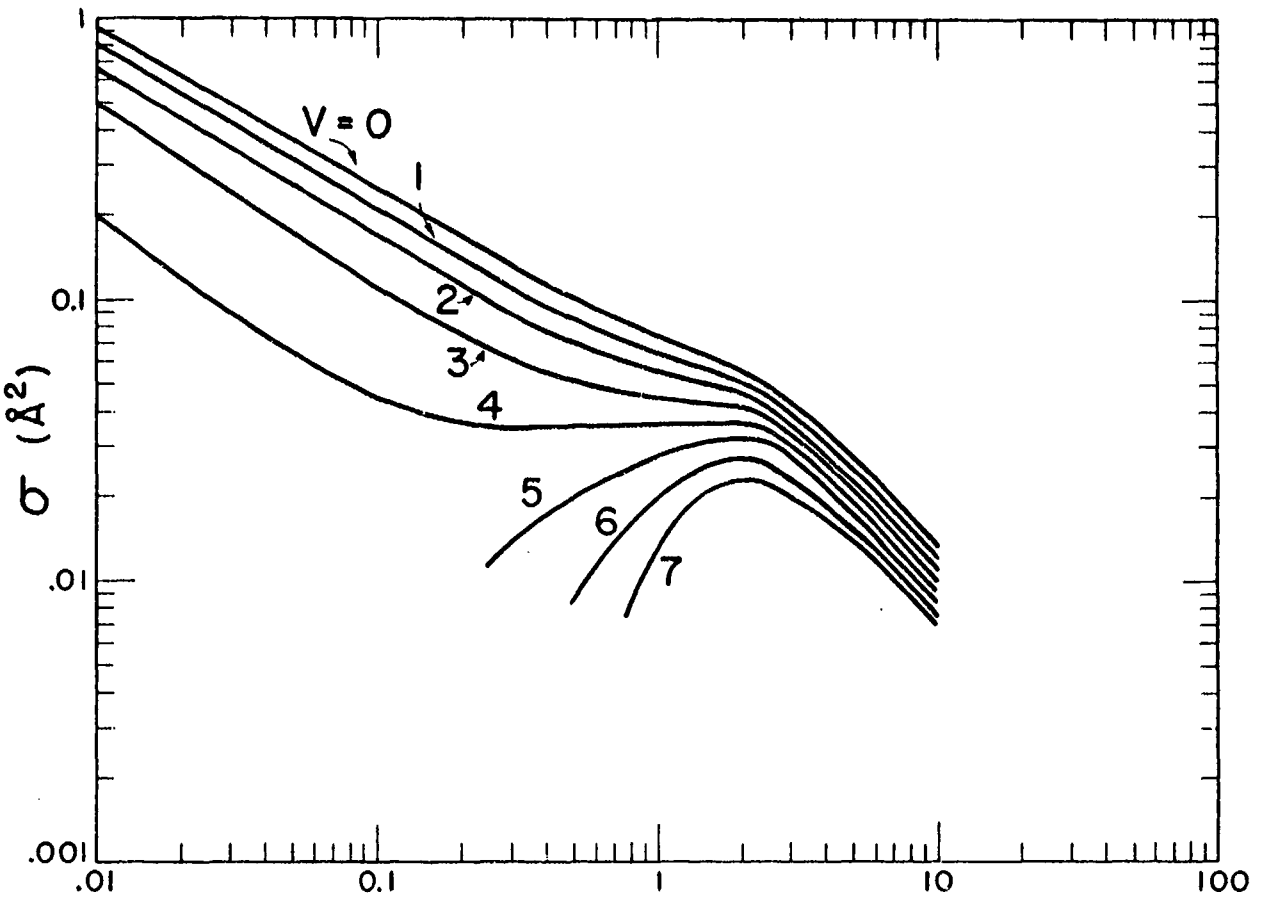

Fig. 18--Vibrational distribution of the products N_2^+ (v=0, 1, ..., 7) + He from the reaction $He^+ + N_2$

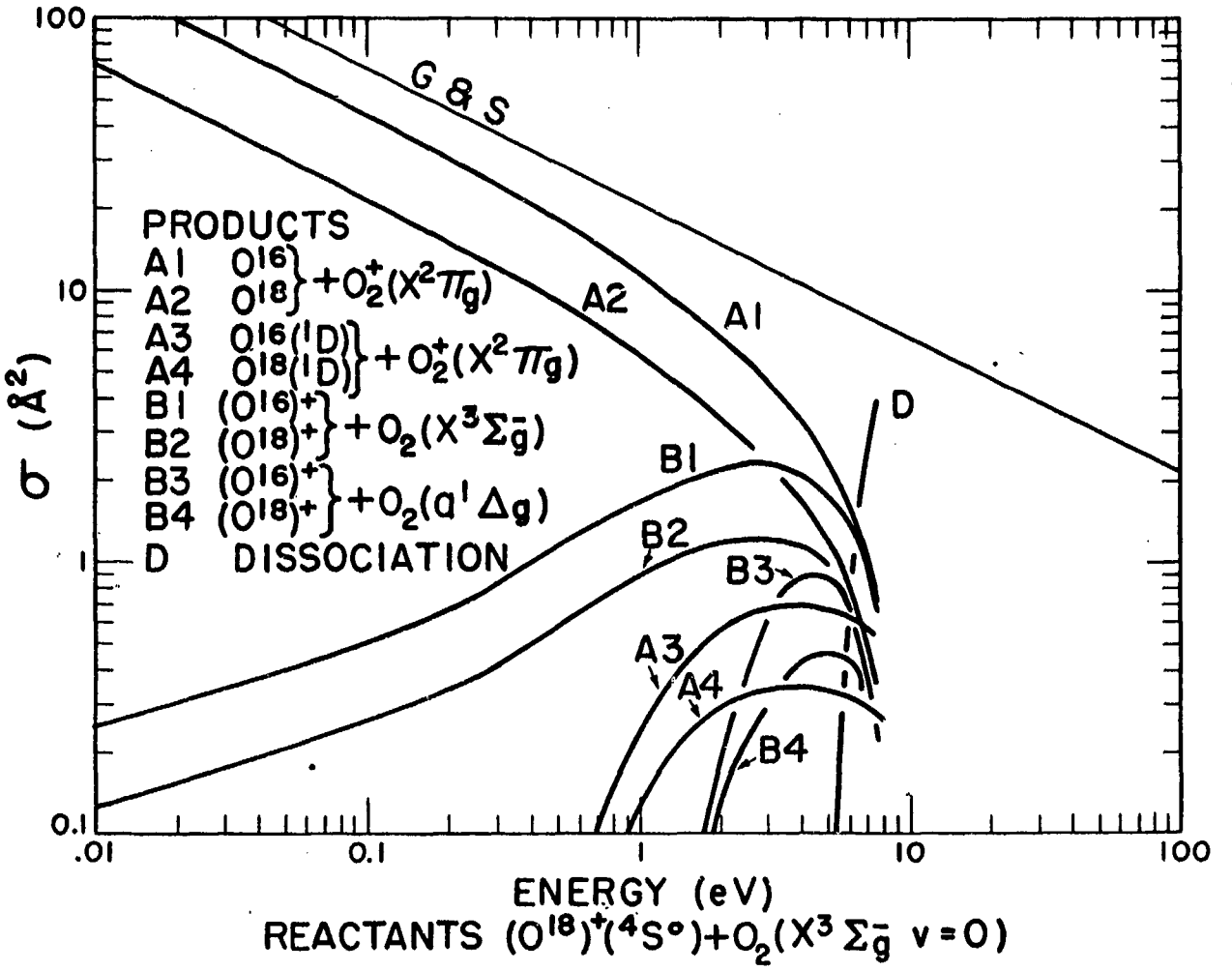

Fig. 19--Distribution of the products O_2^+, $(O^{16}O^{18})^+$, $(O^{16})^+$, and $(O^{18})^+$ from the reaction $(O^{18})^+ + O_2$. The ratios of A1 to A2, A3 to A4, B1 to B2, and B3 to B4 are roughly 2 to 1. This follows from the phase-space theory that $O^{16}O^{18}$ occupies twice the phase space of $O^{16}O^{18}$. That is, reactions of the type $A + B_2 \rightarrow AB + B$ have cross sections 2σ.

REFERENCES AND FOOTNOTES

1. Giese, C. F., and W. B. Maier II, J. Chem. Phys. 39, 739 (1963).

2. Stebbings, R. F., B. R. Turner, and J. A. Rutherford, J. Geophys. Res., to be submitted.

3. Stebbings, R. F., J. A. Rutherford, and B. R. Turner, Planet. Space Sci., to be published.

4. Turner, B. R., M. A. Fineman, and R. F. Stebbings, J. Chem. Phys. 42, 4088 (1965).

5. Gioumousis, G., and D. P. Stevenson, J. Chem. Phys. 29, 294 (1958).

6. Assuming that the induced dipole force is the only long range force.

7. Light, J. C., J. Chem. Phys. 40, 3221 (1964).

8. This theory not only predicts which products are present after reaction, but also the vibrational and electronic states in which they are to be found. The effects of changing the vibrational or electronic state of the reactants can also be determined. This is desirable from the experimental viewpoint since techniques are now in use which enable the experimentor to distinguish among the possible excitation states of the reactants (see Ref. 9).

9. See, for example, Giese, C. F., "Ion-Neutral Reactions," in Advances in Chemical Physics, (Interscience, New York, 1965), Vol. VIII.

10. Integrating over these 12 remaining coordinates would yield the total phase available for a particular three-body combination consisting of a single particle and a diatomic molecule.

11. Pechuckas, P., and J. C. Light, J. Chem. Phys. 42, 328 (1965).

Previous page was blank, therefore not filmed.

REFERENCES AND FOOTNOTES (Cont'd.)

12. Giese, C. F., "Are Resonance Forces Important in Ion-Molecule Reactions?" to be published in Proceedings of Mass Spectrometry Conference, Paris, France, September 14-18, 1964.

13. Arthurs, A. M., and A. Dalgarno, Proc. Roy. Soc. (London) 256A, 540 (1960).

14. See p. 3224 of Ref. 7 for a complete description of this.

15. Gilmore, R. F., Potential Energy Curves for N_2, NO, O_2 and Corresponding Ions, AD-601598, Rand Corporation Memorandum RM-4034-PR on Contract AF-49(638)-700, June 1964.

16. Parkinson, D., Proc. Phys. Soc. (London) 75, 169 (1960).

17. Rothe, E. W., and R. B. Bernstein, J. Chem. Phys. 31, 1619 (1959).

18. See, for example, Herzberg, G., Spectra of Diatomic Molecules, (Van Nostrand, New York, 1950), 2nd ed., p. 101.

19. See Rapp, D., and W. E. Francis, J. Chem. Phys. 37, 2631 (1962), pt. VI, p. 2644.

20. Fehsenfeld, F. C., A. L. Schmeltekopf, and E. E. Ferguson, Planetary Space Sci. 13, 219 (1965).

21. Giese, C. F., private communication. These results are preliminary; final results will be published soon.

22. Bates, D. R., and N. Lynn, Proc. Roy. Soc. (London) 253A, 141 (1959).

23. Schmeltekopf, A. L., F. C. Fehsenfeld, G. I. Gilman, and E. E. Ferguson, to be published.

24. Dr. L. Friedman of the Brookhaven Laboratory, Long Island, New York, has recently pointed out the possibility that the reaction $He^+ + N_2 \rightarrow He + N^+ + N$ could proceed by the intermediary step $(HeN^+)^* + N$. This is under investigation and the results will be published soon.

Defense Threat Reduction Agency
45045 Aviation Drive
Dulles, VA 20166-7517

CPWC/TRC

May 6, 1999

MEMORANDUM FOR DEFENSE TECHNICAL INFORMATION CENTER
ATTN: OCQ/MR WILLIAM BUSH

SUBJECT: DOCUMENT REVIEW

The Defense Threat Reduction Agency's Security Office has reviewed and declassified or assigned a new distribution statement:

- AFSWP-1069, AD-341090, STATEMENT A ~~A~~ waiting for reply
- DASA-1151, AD-227900, STATEMENT A
- DASA-1355-1, AD-336443, STATEMENT A OK
- DASA-1298, AD-285252, STATEMENT A
- DASA-1290, AD-444208, STATEMENT A
- DASA-1271, AD-276892, STATEMENT A
- DASA-1279, AD-281597, STATEMENT A
- DASA-1237, AD-272653, STATEMENT A
- DASA-1246, AD-279670, STATEMENT A
- DASA-1245, AD-419911, STATEMENT A
- DASA-1242, AD-279671, STATEMENT A
- DASA-1256, AD-280809, STATEMENT A
- DASA-1221, AD-243886, STATEMENT A ~~FAD~~
- DASA-1390, AD-340311, STATEMENT A
- ~~DASA-1283, AD-717097, STATEMENT A~~ OK
- DASA-1285-5, AD-443589, STATEMENT A
- DASA-1714, AD-473132, STATEMENT A
- DASA-2214, AD-854912, STATEMENT A
- DASA-2627, AD-514934, STATEMENT A
- DASA-2651, AD-514615, STATEMENT A
- ~~DASA-2536, AD-876697, STATEMENT A~~
- DASA-2722T-V3, AD-518506, STATEMENT A
- DNA-3042F, AD-525631, STATEMENT A
- DNA-2821Z-1, AD-522555, STATEMENT A

If you have any questions, please call me at 703-325-1034.

Ardith Jarrett

ARDITH JARRETT
Chief, Technical Resource Center